

Understanding the role of Al₂O₃ formed during isothermal oxidation in a dual phase AlCoCrFeNi_{2.1} Eutectic High-Entropy Alloy

Mainak Saha

Department of Metallurgical and Materials Engineering, National Institute of Technology,
Durgapur-713209, West Bengal, India

Corresponding author: Mainak Saha

Email address: mainaksaha1995@gmail.com

Phone number: +918017457062

Abstract

In recent times, there has been a significant volume of work on Eutectic High Entropy Alloys (EHEAs) owing to their remarkable castability combined with excellent mechanical properties, which aids in clearing obstacles for their technological applications. One of the most common EHEAs, which has been of huge interest, at present, primarily owing to its solidification and tensile behavior, is AlCoCrFeNi_{2.1}. However, in order to aim for high temperature applications, oxidation behaviour of material is one of the major aspects which needs to be extensively investigated. To this end, the present work aims to study the phases evolved during oxidation at elevated temperatures as high as 950 and 1000°C in AlCoCrFeNi_{2.1} using XRD and also to determine the rate law followed for isothermal oxidation of this alloy at 950 and 1000°C, in order to understand the role of Al₂O₃ phase formed during isothermal oxidation at 950 and 1000°C.

Keywords: Oxidation, Eutectic High-Entropy Alloys (EHEAs), Optical microscopy (OM), X-Ray Diffraction (XRD), Scanning Electron Microscopy (SEM)

1. Introduction

High-entropy alloys (HEAs), or multi-principal-element alloys, differentiate with conventional alloys in that they have at least four principal elements, instead of one or at most, two in the latter. This has led to a paradigm shift in alloy design strategies, and opened a new path for exploration of new materials.

A significant volume of work has been done on understanding solidification behaviour of Eutectic HEAs (EHEAs), especially, due to the excellent castability of these alloys [1-4], arising due to meagre chances of segregation and shrinkage cavities during solidification. Accordingly, if eutectic HEAs with the dual phase FCC + BCC microstructure may be

synthesised, they may be expected to possess the combined advantages of excellent mechanical properties and castability of eutectic alloys coupled with a remarkable strength-ductility optimization arising out of a dual phase FCC+BCC microstructure, especially when both FCC and BCC phases are ordered [1-9]. This has primarily been the ideology behind designing EHEAs, as reported by a number of recent studies. In this context, AlCoCrFeNi_{2.1} is a popular EHEA, in which quite a significant volume of work has been done on correlating the dual phase microstructure comprising of ordered FCC (L1₂) and ordered BCC (B2) phases with the overall solidification behaviour and mechanical response of the alloy, synthesized using different techniques [1-8, 35]. With regard to oxidation, there have been a number of publications which have reported the oxidation behaviour of HEAs. For instance, Daoud et al. [10] examined the oxidation behaviour of Al₈Co₁₇Cr₁₇Cu₈Fe₁₇Ni₃₃, Al₂₃Co₁₅Cr₂₃Cu₈Fe₁₅Ni₁₅, and Al₁₇Co₁₇Cr₁₇Cu₁₇Fe₁₇Ni₁₇ HEAs at 800 °C and 1000 °C in air and reported that at 800 °C, that the alloy with lower Al content forms NiO along with other oxides, namely, Fe₂O₃, Cr₂O₃, and Al₂O₃, unlike at 1000 °C, where the same alloy preferentially forms Cr₂O₃ over Al₂O₃, in contrast to the oxidation behaviour of HEAs with higher Al content, forming Al₂O₃ scales at both temperatures (800 °C and 1000 °C). Holcomb et al. [11] investigated the oxidation behaviour of 8 CoCrFeMnNi-based HEAs, along with different conventional alloys and reported that the Cr and Mn containing HEAs preferentially form both Cr₂O₃ and Mn oxides. Senkov et al. [12] examined the isothermal oxidation behaviour of an arc-melted NbCrMo_{0.5}Ta_{0.5}TiZr refractory HEA (RHEA) at 1000 °C and reported a superior oxidation resistance of the aforementioned alloy as compared to that of similar Nb-based refractory alloys. Similarly, Gorr et al. [13, 14] investigated the influence of Si on the high temperature oxidation behaviour of a 20Nb-20Mo-20Cr-20Ti-20Al HEA and reported that, in general, for HEAs with no Si content, a linear oxide growth rate law is followed with the formation of porous and non-protective oxides whereas, the addition of even 1 at % Si promotes parabolic oxide growth kinetics, to a certain extent, and leads to formation of a thin, continuous and protective Al and Cr rich oxide scale.

However, in view of limited understanding on the oxidation behaviour of AlCoCrFeNi_{2.1} EHEA upto 1200 °C, present work is aimed at understanding the nature of Al₂O₃ phase formed during isothermal oxidation of AlCoCrFeNi_{2.1} EHEA at 950 and 1000 °C.

2. Experiment

Initially, a single sample (in the shape of a button) of AlCoCrFeNi_{2.1} is prepared from Suction Casting of pure components (purity > 99.9%) (on a water-cooled Cu hearth, under Ar inert atmosphere and using Ti as getter). The bar with a rectangular cross-section, so obtained was flipped and remelted multiple times to promote homogeneity and then cut into 8 samples of

average dimensions ~ 10 by 6 mm^2 (approximate thickness $\sim 1.2 \text{ mm}$) using EDM (Electrode Discharge Machining). After standard metallographic polishing, the 1st and 2nd samples were subjected to isothermal oxidation at 1000°C , 500h in a muffle furnace (CWF-1300). The 3rd sample was subjected to isothermal oxidation at 1000°C , 100h in Al_2O_3 crucible, using Kanthal wire as heating element and a static oxidation environment. The 4th and 8th sample were similarly put in the same furnace at 1000 and 950°C , respectively and each of them was taken out after 4, 18, 25, 50 and 100h. Similarly, samples 5 and 6 were oxidised at 950°C , 500h and sample 7 at 950°C , 100h. Phase analysis of the base and oxidized samples was carried out using XRD (X-Ray Diffraction, Bruker) using $\text{Cu}_{k\alpha}$ radiation at 45 mV and 30 mA and, at a scanning rate of $0.02^\circ/\text{min}$ between the scanning range of 20 to 80° and peak fitting was done using Xpert Hi-score analysis software, in order to determine the phases present in the oxidised layer, at different temperatures and time of oxidation. For microstructural characterization, the base sample was etched with aqua regia ($90\% \text{ C}_2\text{H}_5\text{OH} + 10\% \text{ HNO}_3$). The cross sectional area and difference in weight (before and after oxidation) of every sample were measured to determine the oxidation rate law at different temperatures of oxidation.

3. Results and discussions

3.1 Phase analysis during oxidation using X-Ray Diffraction (XRD)

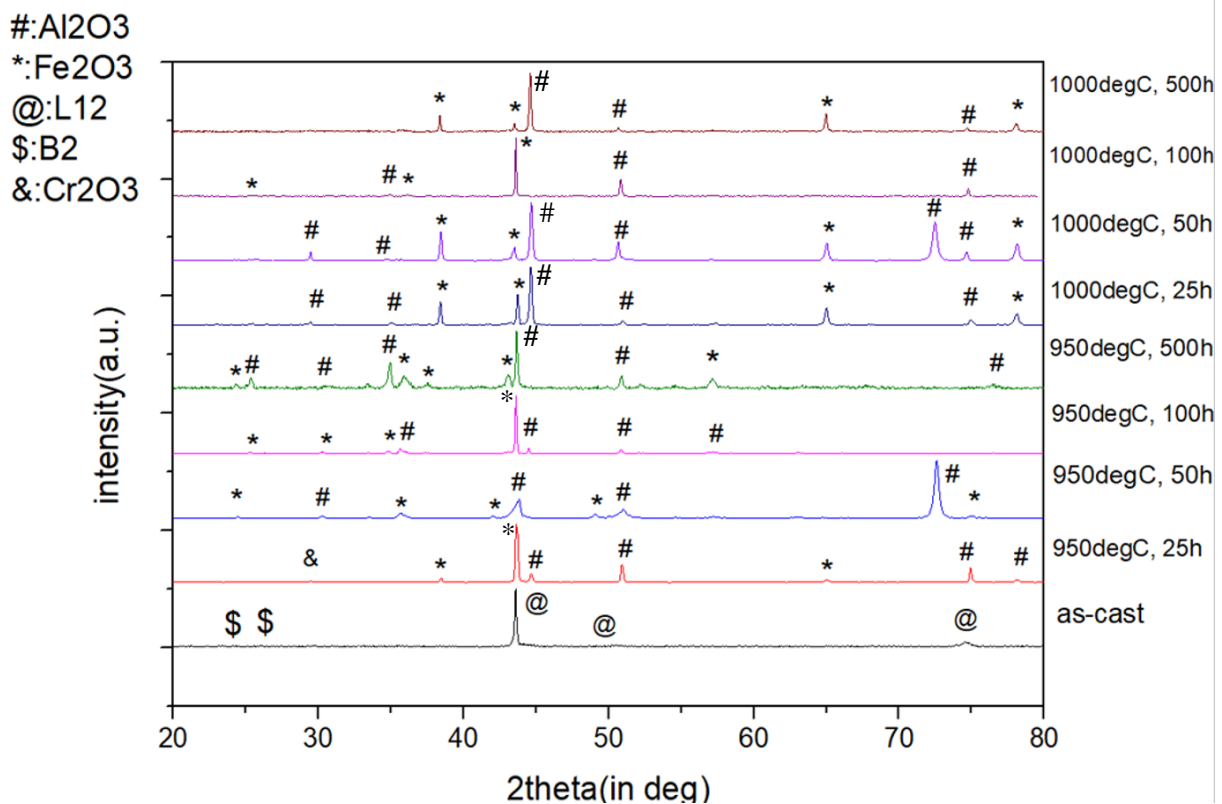


Fig 1. Stacked XRD plots of as-cast (at the bottom, marked as black) to oxidised samples at different temperatures and time of isothermal oxidation (marked as red, blue, pink, green, deep blue, violet indigo and maroon).

Fig. 1 shows the X-Ray diffractograms of as-cast along with oxidised samples. The variation in terms of angular Wavenumber (k), with the exception of 1000°C, 100h sample, is observed from 1 to 5. Whereas, the variation in the same quantity is observed between 2 and 5 in 1000°C, 500h sample. Moreover, It is evident (from Fig. 1) that in as-cast sample, there is a dual-phase microstructure comprising of B2 (ordered BCC) and L1₂ (ordered FCC) phases (lattice parameters: 3.6011 Å and 5.9375 Å, respectively), with the most intense (111) superlattice peak at $2\theta = 43.5^\circ$, corresponding to L1₂ phase. Besides, it is also observed that in as-cast sample, there are more peaks of L1₂ phase as compared to that of B2. After isothermal oxidation at varying temperatures and times of oxidation till 1000°C, 500h, there are three phases detected by XRD analysis: L1₂, Al₂O₃ and Fe₂O₃. After 25h of isothermal oxidation at 950°C, Cr₂O₃ phase is also observed. However, after 100h of oxidation, it is clearly observed that there are 2 oxides present (similar to that observed after isothermal oxidation at 950°C for 25h) namely, Al₂O₃ and Fe₂O₃ phases, with the most intense (113) peak of Fe₂O₃ at $2\theta = 43.5^\circ$, indicating that Fe₂O₃ is the predominant oxide phase at 950°C, 100h sample. Unlike Al₂O₃, Fe₂O₃ phase forms a non-protective oxide layer but the exact information about oxides may be gained only by looking at cross-sections using SEM [15-17] which will be taken up in subsequent publications. After 500h of isothermal oxidation at 950°C, the most intense (113) peak corresponds to that of Al₂O₃ at exactly $2\theta = 43.5^\circ$ indicating that Al₂O₃ phase forms the matrix with 2nd phase as Fe₂O₃, similar to the microstructure after 50h of oxidation at 950°C. Besides, after 1000°C, 100h of isothermal oxidation, the volume fraction determination of individual phases based on the relative intensities of XRD peaks clearly indicates that Fe₂O₃ phase forms the matrix and Al₂O₃ forms the 2nd phase in a dual phase Al₂O₃ + Fe₂O₃ microstructure, similar to that in samples oxidized at 950°C for 25 and 100h. However, after 500h of isothermal oxidation at 1000°C, the most intense (113) peak of Al₂O₃ with its position (2θ) shifted slightly to the right i.e. at $2\theta = 43.7^\circ$, indicates a dual phase microstructure comprising of Al₂O₃ (matrix) and Fe₂O₃ phases, similar to that in samples after oxidation at 950°C for 50 and 500h and that after oxidation at 1000°C for 25 and 50h although the detailed phase analysis, is beyond the scope of discussion of the present work, as because XRD, being a bulk characterization technique, cannot detect phases with vol. fraction of less than 0.05.

3.2 Microstructural characterization of as-cast sample

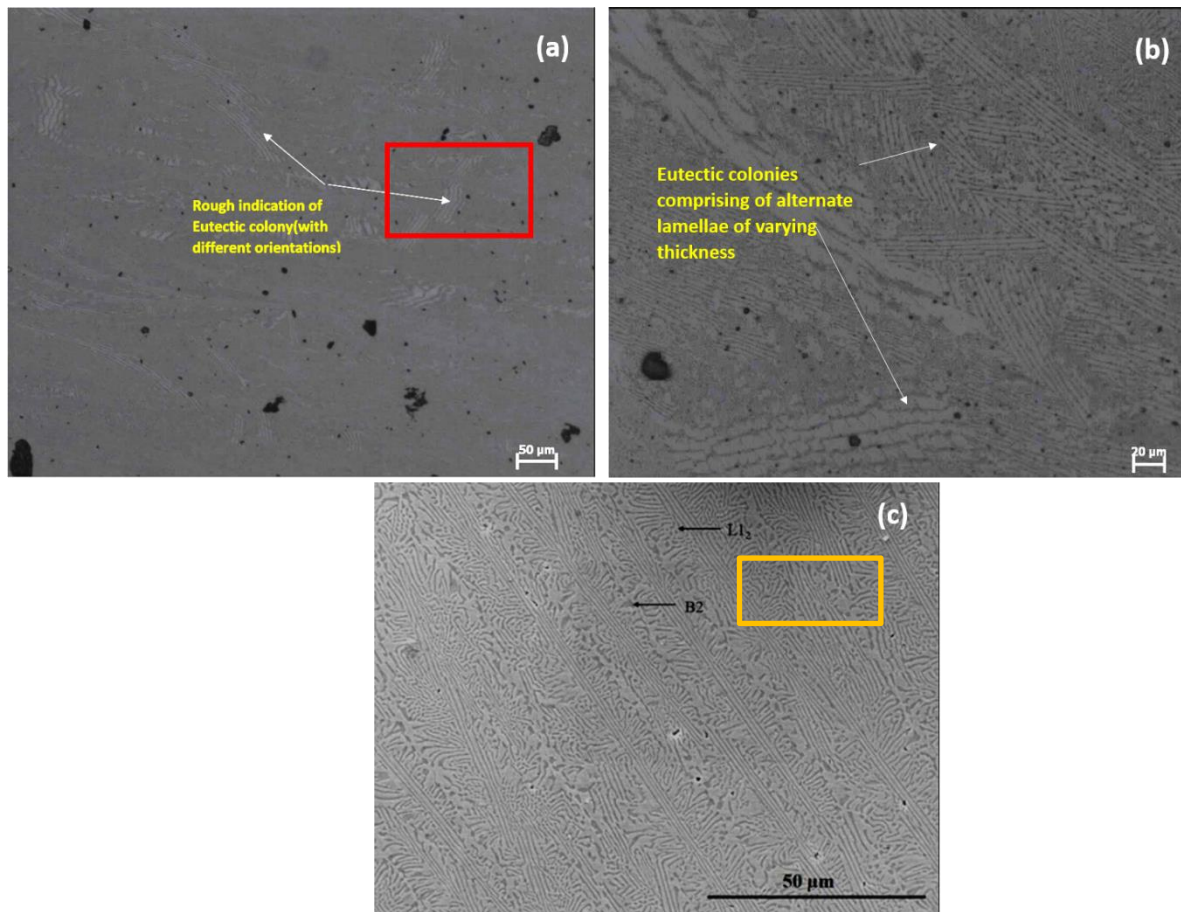


Fig. 2 As-cast sample: **(a)** Optical image (100x), **(b)** Optical image (500x) of the region highlighted with a red outlined enclosure in part **(a)**; and **(c)** SEM image (3000x) showing eutectic colonies with alternate lamellae (of various thickness) of L_{12} and B2 phases (enclosed within orange outlined rectangular box in part **(c)**)

Both optical and SEM images reveal eutectic colonies with alternate lamellae (of various thickness) of L_{12} and B2 phases. Based on image analysis using ImageJ software, the average thickness of L_{12} phase is found to be nearly $1 \mu\text{m}$ whereas that of B2 lamella is found to be nearly $1.2 \mu\text{m}$. Besides, the phase fraction of L_{12} and B2 phases (based on variation in contrast) in the as-cast microstructure is also found to be 0.89 and 0.11 respectively from Figs. **2(a-c)**, similar to that inferred from the XRD of as-cast sample in Fig. 1.

3.3 Isothermal oxidation kinetics at 950°C and 1000°C

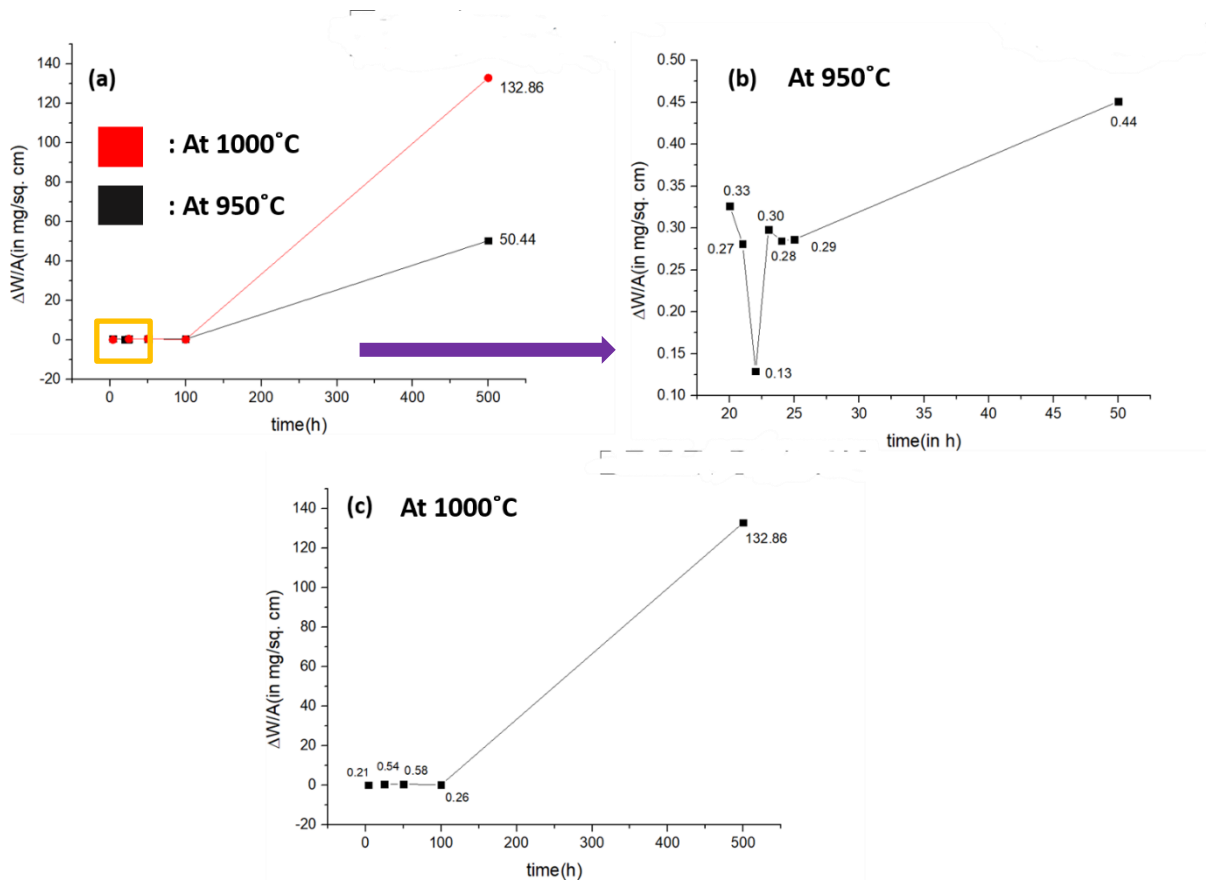


Fig. 3 (a) Comparative Isothermal oxidation plots of AlCoCrFeNi_{2.1} EHEA at 950 and 1000°C between 4h and 500h of oxidation, (b) Isothermal oxidation plot of AlCoCrFeNi_{2.1} EHEA at 950°C between 4h and 50h of oxidation (drawn as subplot of part (a)) and (c) Isothermal oxidation plot of AlCoCrFeNi_{2.1} EHEA at 1000°C (plotted separately for a higher level of clarity) between 4h and 500h of oxidation.

From the previous studies of oxidation behaviour of AlCoCrFeNi_{2.1} EHEA, [1-8], it has been reported that at elevated temperatures between 900 and 1300°C, the weight loss curve for oxidation initially shows a parabolic nature, which saturates with higher periods of oxidation. Fig. 3(a), its subplot (Fig. 3(b)) and Fig. 3(c) indicate that irrespective of considerable fluctuations in these weight loss curves due to reasonable amounts of spallation, a linear rate law is observed at both 950 and 1000°C, with increase in time of oxidation at both these temperatures. Combining the observation on the phase fraction of Al₂O₃ and Fe₂O₃ phases (Fig. 1) with the weight loss curves (Figs. 3(a-c)), it may be inferred that a slightly higher volume fraction of Al₂O₃ phase (in a dual phase Al₂O₃ + Fe₂O₃ microstructure) after isothermal oxidation at 1000°C for 500h (that that after oxidation at 950°C for 500h) leads to a significantly higher amount of weight loss than that after isothermal oxidation at 950°C for 500h. This further provides an indication that Al₂O₃ scale formed during oxidation at elevated temperatures in

AlCoCrFeNi_{2.1} EHEA aids in further oxidation unlike the reported nature of Al₂O₃ scale [1-4]. However, the detailed microstructural investigation supporting the present claim on the nature of Al₂O₃ scale formed during prolonged periods of high temperature oxidation of AlCoCrFeNi_{2.1} EHEA, will be discussed in subsequent publications.

4. Conclusions

1. During isothermal oxidation at 950 and 1000°C, for oxidation periods ranging from 25 to 500h, AlCoCrFeNi_{2.1} EHEA (with a dual phase L₁₂ + B₂ microstructure) shows a dual phase Al₂O₃ + Fe₂O₃ microstructure.
2. At 950°C, there is phase reversion from Al₂O₃ to Fe₂O₃ when oxidation is performed till 50h. However, Fe₂O₃ reverts back to Al₂O₃ when oxidation is performed at 950°C for 100 and 500h. Similarly, At 1000°C, there is phase reversion from Al₂O₃ to Fe₂O₃ when oxidation is performed till 100h followed by a re-reversion from Fe₂O₃ to Al₂O₃ phase for oxidation till 500h at 1000°C.
3. Irrespective of considerable fluctuations in weight loss curves due to reasonable amounts of spallation, a linear rate law is observed at both 950 and 1000°C, with increase in time of oxidation at both these temperatures from 4h till 500h.
4. Al₂O₃ scale formed during oxidation at elevated temperatures in AlCoCrFeNi_{2.1} EHEA aids in further oxidation unlike the reported nature of Al₂O₃ scale.

Acknowledgement

MS is thankful to the Department of Metallurgical and Materials Engineering, NIT Durgapur, for carrying out the work.

References

- [1]. Wani IS., Bhattacharjee T, Sheikh S, Lu YP., Chatterjee S., Bhattacharjee PP, Guo S & Tsuji N: Ultrafine-Grained AlCoCrFeNi_{2.1} Eutectic High-Entropy Alloy. Mater. Res. Lett. 2016; 1-6.
- [2]. Yiping L., Xuzhou G., Li J., Zongning C. , Tongmin W. , Jinchuan J. , Huijun K. , Yubo Z. , Guo S. , Haihui R. , Yonghao Z. , Zhiqiang C. , Tingju L.: Directly cast bulk eutectic and near-eutectic high entropy alloys with balanced strength and ductility in a wide temperature range. Acta Mater. 2017; 124; 143-150.
- [3]. Wani IS., Bhattacharjee T, Sheikh S, Lu Y, Chatterjee S, Guo S, Bhattacharjee PP and Tsuji N, Effect of severe cold-rolling and annealing on microstructure and mechanical properties of AlCoCrFeNi_{2.1} eutectic high entropy alloy. IOP Conf. Series: Mat. Sci. and Eng.

2017; 194 1-5.

- [4]. Wani IS., Bhattacharjee T., Sheikh S., Clark IT., Park M.H., Okawad T., Guo S., Bhattacharjee PP., Tsuji N., Cold-rolling and recrystallization textures of a nano-lamellar AlCoCrFeNi_{2.1} eutectic high entropy alloy. *Intermetallics*. 2017; 84; 42-51.
- [5]. Xuzhou G., Yiping L., Bo Z., Ningning L., Guanzhong W., Gang S., Jizi L., Yonghao Z., Microstructural origins of high strength and high ductility in an AlCoCrFeNi_{2.1} eutectic high-entropy alloy. *Acta Mater*. 2017; 141;59-66.
- [6]. Yaoli Z., Xinguang W., Jinguo L., Yaqi H., Yiping L., Xiaofeng S., Deformation mechanism during high-temperature tensile test in an eutectic high-entropy alloy AlCoCrFeNi_{2.1}, *Mat. Sci & Eng. A*. 2018; 724; 148–155.
- [7]. Ding P., Aiqin M., Xiang Z., Xia J., Biao W., Min Liu , Xiaolong G., Preparation, characterization and properties of multicomponent AlCoCrFeNi_{2.1} powder by gas atomization method. *J.Alloys Compd*. 2017; 721; 609-614.
- [8]. Bhattacharjee T., Zheng R., Chong Y., Sheikh S., Guo S., Clark IT., Okawa T., Wani IS., Bhattacharjee PP., Shibata A., Tsuji N., Effect of low temperature on tensile properties of AlCoCrFeNi_{2.1} eutectic high entropy alloy. *Mat. Chem. Phys*. 2018; 210; 207-212.
- [9]. Jichao J., Xiuyan L., High temperature oxidation behaviour of AlCuTiFeNiCr high-entropy alloy. *Adv. Mat. Res*. 2013; 652-654; pp 1115-1118.
- [10]. Daoud, H.M.; Manzoni, A.M.; Volkl, R.; Wanderka, N.; Glatzel, U. Oxidation behavior of Al₈Co₁₇Cr₁₇Cu₈Fe₁₇Ni₃₃, Al₂₃Co₁₅Cr₂₃Cu₈Fe₁₅Ni₁₅, and Al₁₇Co₁₇Cr₁₇Cu₁₇Fe₁₇Ni₁₇ compositionally complex alloys (high-entropy alloys) at elevated temperatures in air. *Adv. Eng. Mater*. 2015, 17, 1134–1141.
- [11]. Holcomb, G.R.; Tyleczak, J.; Carney, C. Oxidation of CoCrFeMnNi high entropy alloys. *JOM* 2015, 67, 2326–2339.
- [12]. Senkov, O.N.; Senkova, S.V.; Dimiduk, D.M.; Woodward, C.; Miracle, D.B. Oxidation behavior of a refractory NbCrMo_{0.5}Ta_{0.5}TiZr alloy. *J. Mater. Sci*. 2012, 47, 6522–6534. 27.
- [13]. Gorr, B.; Azim, M.; Christ, H.J.; Mueller, T.; Schliephake, D.; Heilmaier, M. Phase equilibria, microstructure, and high temperature oxidation resistance of novel refractory high-entropy alloys. *J.Alloys Compd*. 2015,624, 270–278.
- [14]. Gorr, B.; Mueller, F.; Christ, H.J.; Mueller, T.; Chen, H.; Kauffmann, A.; Heilmaier, M. High temperature oxidation behaviour of an equimolar refractory metal-based alloy 20Nb-20Mo-20Cr-20Ti-20Al with and without Si addition, *J. Alloys Compd*. 2016, 688, 468–477.
- [15]. Butler TM. and Weaver ML., Influence of Annealing on the Microstructures and Oxidation Behaviors of Al₈(CoCrFeNi)₉₂, Al₁₅(CoCrFeNi)₈₅, and Al₃₀(CoCrFeNi)₇₀ High-Entropy Alloys, *Metals* 2016, 6, 222, 2-11.
- [16]. Butler TM. and Weaver ML., Oxidation behaviour of arc melted AlCoCrFeNi multi-component High-Entropy Alloy, *J. Alloys Compd*, 674, 2016, 229-244.

[17]. Butler, T.M.; Alfano, J.P.; Martens, R.L.; Weaver, M.L. High-temperature oxidation behavior of Al-Co-Cr-Ni-(Fe or Si) multicomponent high-entropy alloys. JOM 2015, 67, 246–259.

